Desalination and Water Treatment
www.deswater.com
doi: 10.5004/dwt.2022.28806

273 (2022) 281–291
October

Fe-doped TiO_2 sonocatalytic process for removal of ofloxacin and ciprofloxacin from aqueous solution

Abbas Khalili[a], Hossein Kamani[b,*], Reza Haji Seyed Mohammad Shirazi[a], Amir Hessam Hassani[a]

[a]*Department of Natural Resources and Environment, Science and Research Branch, Islamic Azad University, Tehran, Iran, emails: khaliliamir96@gmail.com (A. Khalili), r-shirazi@srbiau.ac.ir (R.H.S. Mohammad Shirazi), Ahhassani@srbiau.ac.ir (A.H. Hassani)*
[b]*Health Promotion Research Center, Zahedan University of Medical Sciences, Zahedan, Iran, Tel. +989155412919; Fax: +985433295837; emails: hossein_kamani@yahoo.com (H. Kamani)*

Received 19 April 2022; Accepted 26 July 2022

ABSTRACT

The use of antibiotics in veterinary medicine and medical applications has increased widely, and the possibility of contamination of water sources with such compounds has increased, which causes adverse effects such as increased bacterial resistance and gastrointestinal disorders in humans and other organisms. In this study, Fe-doped TiO_2 nanoparticles were synthesized by the simple sol-gel method. Then, the sonocatalytic efficiency of these synthesized nanoparticles in the removal of the ofloxacin and ciprofloxacin was investigated. Scanning electron microscopy (SEM), energy dispersive x-ray spectroscopy (EDX), X-ray diffraction (XRD), and diffuse reflectance spectroscopy (DRS) analyses were used to characterize the nanoparticles. The effect of different independent parameters including pH (3–11), initial concentration of ofloxacin and ciprofloxacin (50–200 mg/L), and nanoparticle concentrations (200–700 mg/L) at different times (15–60 min) were examined for sonocatalytic removal of ofloxacin and ciprofloxacin. The results showed that the synthesized nanoparticles are very small and have a size in the range of nanometers. EDX showed the presence of Ti, Fe, and O elements in the structure of synthesized nanoparticles. The peaks of 25.68, 37.75, 48.28, 54.27, and 55.24, which are marked inside the figure of XRD, confirm the crystal structure of the anatase phase. Doping iron in the structure of titanium dioxide causes the absorption wavelength to shift to higher wavelengths and get closer to the visible region. The maximum removal efficiency and the highest constant rate of reaction for ofloxacin and ciprofloxacin at the initial concentration of 50 mg/L, the nanoparticles dosages of 700 mg/L at the reaction time of 60 min, and ultrasound frequency of 35 kHz were obtained at pH values of 3 and 9, respectively. In this study, the degradation mechanism of the process and stability of synthesized nanoparticles were also investigated. The results showed that the nanoparticles have good stability and the use of the sonocatalytic process is an effective method to remove ofloxacin and ciprofloxacin from aqueous solutions.

Keywords: Fe-doped TiO_2; Sonocatalyst; Antibiotic; Sol–gel; Kinetic

1. Introduction

Today, the presence of drugs and personal care products, including anti-inflammatory compounds, antibiotics, and hormones in aqueous media, has received much attention and has become a concern as emerging pollutants. Despite the low concentrations detected in water sources, it can have effects on ecosystems and human health. These

* Corresponding author.

effects include increased allergies in humans, the spread of antibiotic-resistant bacteria, upsetting the environmental balance, and causing unforeseen effects on humans and animals. On the other hand, constant contact with antibiotics can increase the number of resistant bacterial species in the environment [1–3].

Fluoroquinolones are the strongest group of antibiotics that are very useful in the treatment of respiratory and urinary tract infections. However, they have also harmful effects, including effects on the central nervous system. Ofloxacin and ciprofloxacin, as the most commonly used fluoroquinolone antibiotics, are widely found in various aquatic environments, including wastewater treatment plant effluents, pharmaceutical effluents, hospital effluents, drinking water, rivers, and seas [4,5].

Degradation of this type of compound is an important biological challenge due to its complex structure and very low biodegradability [6]. Therefore, new processes with cost-effective methods are needed to treat antibiotics, one of which is sonocatalyst. The main mechanism of the ultrasonic process in the oxidation of pollutants is based on the formation of very small cavities or micro-bubbles that are the result of the phenomenon of sound cavitation in water. When cavity explosion occurs, a phenomenon of photoluminescence occurs which is accompanied by light radiation and has a wavelength of less than 375 nm, this path is similar to the photocatalytic process. Furthermore, when the photocatalytic phenomenon occurs in the continuation of the sonocatalytic process, the band gap reducing helps the photocatalytic phenomena to occur more easily and the electron is easily transferred from the valence layer to the conducting layer [7]. The holes created in the water have a high temperature and pressure, which eventually leads to the formation of OH and OOH free radicals in the solution. These radicals penetrate the water and cause the oxidation of organic compounds, but the use of this process alone requires time and the high power of the waves [8,9].

In the study of Hapeshi et al. conducted for the degradation of ofloxacin in the secondary treated effluent, the removal efficiency using the sonolysis process was reported to be 8% while it was 62% using the sonocatalytic process [10]. Therefore, semiconductor nanocatalysts such as TiO_2 are used simultaneously with the application of ultrasound. Titanium dioxide nanoparticles are widely used due to their non-toxicity, cheapness, high chemical stability, and catalytic activity without the production of secondary pollutants [9,11,12]. However, the use of TiO_2 is severely limited due to the wide band gap (3.2 electron volts) and low quantum efficiency. Therefore, to increase the catalytic power of TiO_2, modification methods such as doping with metal and non-metallic ions, sensitization with polymers, and creating heterogeneity with other semiconductors are used [6]. Among the above-methods, doping with metal ions has had the best results. In a study conducted by Wang et al., sonocatalytic effect of Fe-doped TiO_2 for the degradation of Fuchsine azo dye, showed that the sonocatalytic activity of Fe-doped TiO_2, TiO_2, and ultrasound after 60 min of irradiation have efficiencies 58, 37, and 16%, respectively [13]. Among different types of metals in ion doping technique, Fe^{3+} has been proposed as a suitable element due to the high similarity of Fe^{3+} radius (0.645 angstroms) to Ti^{4+} (0.604 angstroms) and easy connection to titanium dioxide crystal lattice (inhibition of holes and electron recombination) [6,8,14–16].

So far, several methods have been used to synthesize nanoparticles. It has been reported that different methods have different results, and even in a particular method, the use of various amounts of raw materials leads to the production of particles of different sizes. On a laboratory scale, the sol–gel process is more commonly used to synthesize different types of nanoparticles [6]. The sol–gel method is a wet chemical method that is performed at room temperature. Typically, the sol–gel process consists of five steps including hydrolysis of alkoxy precursors, formation of particle or polymer sol containing inorganic materials, formation of a gel by evaporation of volatile compounds and solvent, drying at room temperature to obtain a dense mineral network, calcination at very high temperatures to remove organic matter and crystallize solids [17].

In the literature review, it was found that the removal of the ofloxacin and ciprofloxacin from aqueous media has been studied using various methods of oxidation and advanced oxidation such as ozonation process, photo-Fenton, photocatalyst, etc.; however, there is no study on the sonocatalysis process using Fe-doped TiO_2 nanoparticles in the removal of these contaminants. The present study investigates the effect of parameters affecting the sonocatalytic process using Fe-doped TiO_2 nanoparticles in the removal of the above contaminants. In summary, the purpose of this study can be stated as follows: Synthesis of Fe-doped TiO_2 nanoparticles by sol–gel method and evaluation of its physical and chemical properties, evaluation of the performance of synthesized nanoparticles in the degradation of ofloxacin and ciprofloxacin, determination of the effect of different process parameters on removal rate, evaluation of process kinetics, assessment of reusability and stability of synthesized nanoparticles, and determination of final products obtained from the degradation of ofloxacin and ciprofloxacin.

2. Materials and methods

This research is an experimental-laboratory study that was performed as a batch system in the laboratory. To evaluate the removal efficiency of antibiotics by synthesized nanoparticles and sonocatalytic method, OFAT (One Factor at a Time Method) method was used and the total number of samples using this method was 84.

Chemicals used include tetraisopropyl orthotitanate (≥98%), nitric acid (65%), iron(III) nitrate nonahydrate (≥98%), 2-propanol, sulfuric acid (95–97%) and sodium hydroxide (98%), which were purchased from Merck, Germany. Ofloxacin and ciprofloxacin were brought from Sigma-Aldrich.

2.1. Synthesis of Fe-doped TiO_2 and TiO_2 nanoparticles

In this study, the sol-gel method was used for synthesis of Fe-doped and non-doped TiO_2 nanoparticles. To prepare of nanoparticles, 0.08 g iron nitrate, 10 mL 2-propanol alcohol and 0.02 mL nitric acid were poured into a flat bottom glass balloon and were stirred for 15 min on

a magnetic stirrer to mix thoroughly (solution No. 1). In another Erlenmeyer flask, 3 mL titanium tetraisopropoxide was mixed in 20 mL 2-propanol for 15 min to form a uniform and clear solution (solution No. 2). Then, solution No. 1 was added dropwise to the solution of container No. 2, which was mixing on a magnetic stirrer. After mixing both solutions (solutions No. 1 and No. 2) for 30 min and forming a clear sol inside the balloon, the balloon containing clear sol was placed in the laboratory at room temperature for 5 h. Semi-transparent gel was obtained which had good resistance and the adhesion. The resulting gel was placed in an oven at 80°C for 24 h to dry. Then, the resulting dry powder, after washing several times with twice distilled water, was calcined at 500°C in an oven for 1 h to prepare crystalline nanoparticles and to obtain powder nanoparticles [9].

2.2. Characteristics of reactor

Ultrasonic cleaner (ultrasonic bath): Digital Ultrasonic device (model: Elmasonic Tl-H, made in Germany) equipped with a stainless steel tank with a useful volume of 3.5 L and dimensions of 300 × 340 × 370 with a frequency of 35 kHz was used in the present study.

2.3. Sonocatalytic degradation experiments

The desired concentrations of ofloxacin and ciprofloxacin (50–100–200 mg/L) were prepared by diluting a certain amount of stock solution of ofloxacin and ciprofloxacin in a volume of 250 ml, and the pH of the solution was regulated using 0.1 N sodium hydroxide and sulfuric acid, and a certain amount of Fe-doped TiO_2 nanoparticles was then added to the solution. Sampling was performed at different time intervals from the suspension irradiated with ultrasonic waves. After separating the nanoparticles from the process solution, the amount of light absorbed by the contaminant remaining in the solution was read using a spectrophotometer at the specific wavelength, and the removal efficiency was determined using the following formula.

$$\text{removal efficiency} = \frac{\left(C_0 - C_e\right)}{C_0} \times 100 \quad (1)$$

where C_0: initial concentration of antibiotic and C_e: final concentration of antibiotic.

3. Results and discussion

3.1. SEM analysis

SEM analysis was performed using a SEM FEI Quanta 200 device equipped with EDX. Fig. 1 shows the images of Fe-doped TiO_2 catalyst particles. As shown in Fig. 1, the synthesized particles are almost uniform, and no significant aggregates are observed in them. The synthesized particles are very small and have a size in the range of nanometers.

3.2. EDX analysis

Fig. 2 shows the EDX spectrum diagram for Fe-doped TiO_2 nanoparticles. As shown in the figure, the spectrum of the participating elements confirms the presence of Ti, Fe, and O elements in the structure of the synthesized sample. The mass percentage of elements in the synthesized sample is presented in Table 1. The results of Table 1 show the presence of the above elements in the structure of synthesized nanocatalyst and also confirm the doping process of synthesized nanoparticles.

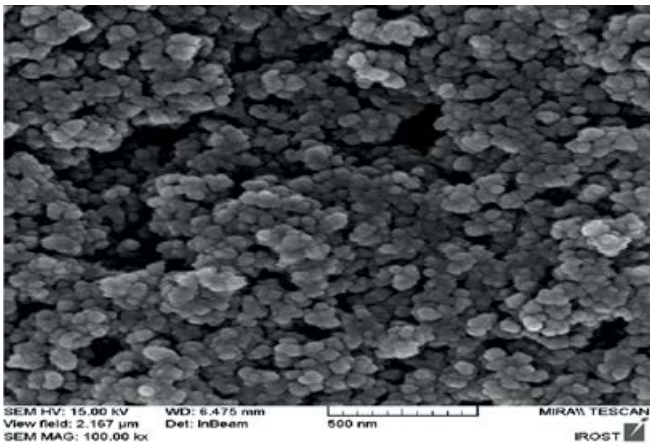

Fig. 1. SEM image of synthesized Fe-doped TiO_2 nanoparticles.

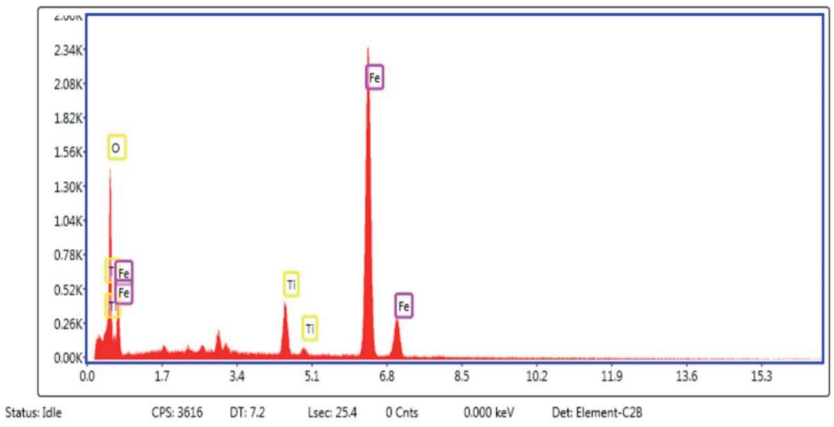

Fig. 2. EDX spectra for Fe-doped TiO_2 nanoparticles.

Table 1
Mass percentage of elements in nanoparticle synthesized using EDX analysis

Sample elements	Fe-doped TiO_2
O	21.7
Ti	72.1
Fe	6.2
Total	100

3.3. XRD analysis

In order to determine the crystal structure, to estimate the size of the formed crystals and determine the phase of the crystal structure of nanoparticles, X-ray diffraction (XRD) spectroscopy was used. The XRD is widely used to identify unknown crystalline solid samples and 3–5 g are usually used to do that. The operation of the XRD device is so that the X-ray is irritated on the crystal at different angles (θ). As a result of this radiation and the impact of the beam on the atoms, the radiation is reflected or so-called diffracted. The device model used is Bruker D8 Advance. Fig. 2 shows the XRD pattern of TiO_2 and Fe-doped TiO_2 nanoparticles at a distance of 10–80° (2q).

Crystal size in the synthesized nanoparticle samples was calculated using the Debye–Scherrer equation according to the following formula [9]:

$$D = \frac{K\lambda}{\beta\cos\theta} \tag{2}$$

where D is the average diameter of the crystallite size (nm), K is the refractive index of the crystal (which is usually constant and equal to 0.9), λ is the X-ray wavelength used for XRD analysis (in this study, the wavelength is 1.5441 A), θ is diffraction angle in terms of degree and β is the full-width at half maximum (FWHM).

Fig. 3 shows that the XRD pattern of Fe-doped TiO_2 nanoparticles has a large and sharp peaks, which are indicative of the fine crystal structure of the synthesized nanoparticles. The peaks of 25.68, 37.75, 48.28, 54.27, and 55.24, which are marked inside the figure, confirm the crystal structure of the anatase phase.

As shown in Fig. 3, the positions of the peaks on the X-axis are approximately the same, and no significant peaks were observed in the Fe-doped TiO_2 nanoparticles after the doping process, which confirms that the crystal structure of TiO_2 has not changed significantly. The absence of a significant peak after the doping process could be due to the fact that the amount of iron is less than the detection limit, or the device is not sensitive. On the other hand, the ionic radii of Ti^{4+} and Fe^{3+} are almost identical to each other, so it is possible that a number of titanium dioxide lattice sites are occupied by iron ions [18,19]. On the other hand, doping of TiO_2 nanoparticles has led to changes in reflections at lower angles, which may be due to the replacement of Ti^{4+} ions with slightly larger Fe^{3+} ions. Kamani et al. obtained similar results and reported that the widening of the peaks and the change of reflections at lower angles changed the absorption edge to the visible region [7].

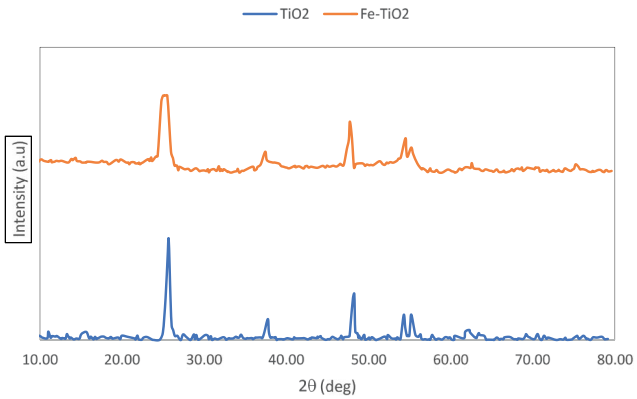

Fig. 3. XRD pattern of TiO_2 and Fe-doped TiO_2 nanoparticles.

3.4. DRS analysis

DRS analysis has been used to investigate the reduction in band gap size after doping of doped elements in the structure of synthesized nanoparticles (DR-Ar-2016 model). A spectrophotometer, or spectroscopy device, examines actually the interaction of light with matter. The basis of this technique is irradiation of light on the surface of a powder material and the measurement of the diffusion reflectance is compared to the standard sample. By measuring the diffusion reflectance, the optical properties of powder materials can be evaluated. Fig. 4a shows that the absorption spectra for two samples synthesized are in the wavelength range of 250–800 nm. In addition to determining the absorption spectrum, it is possible to quantitatively calculate the band gap of nanoparticles using data obtained from DRS analysis and using the Kubelka–Munk Function and Tauc's Method, followed by plotting the $\alpha h\nu^{1/2}$ against absorbed photon energy in terms of electron volts (hv).

$$(\alpha h\nu) = A\left(h\nu - E_g\right)^r \tag{3}$$

where α is the absorption coefficient, h is the Planck constant, v is the light frequency, A is the absorption constant, E_g is the nanoparticle energy gap, and r is the optical transmission process.

According to Fig. 4a, TiO_2 nanoparticles did not show significant light absorption in the visible spectrum (l>400), and the absorption threshold for it was at the beginning of the wavelengths of the visible spectrum (401 nm). However, doping iron in the structure of titanium dioxide has shifted the absorption wavelength to larger wavelengths and closer to the visible region. The reduction in band gap energy is also due to the reaction of the 3d orbital of titanium and the d-orbital of iron; the placement of iron in the structure of titanium dioxide and between titanium dioxide atoms leads to the production of an additional energy balance between the valence layer and the conduction layer of titanium dioxide nanoparticles. The doped iron element in the structure of titanium dioxide acts as an intermediate energy level, reducing the band gap and changing the absorption of light towards the visible region [19–21].

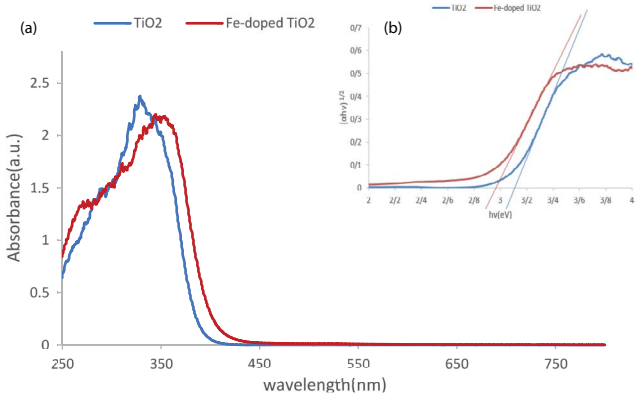

Fig. 4. (a) Visible light absorption spectrum – ultraviolet (DRS) spectrum of TiO_2 and Fe-doped TiO_2 particles and (b) Tauc's plots to calculate the band gap of synthesized nanoparticles.

As shown in Fig. 4b, after doping the elements into the titanium dioxide structure, the band gap energy was reduced from 3.08 to 2.9 eV in 2% molar samples. The reduction in band gap energy in Fe-doped TiO_2 may be due to doping the iron in the structure of titanium dioxide. Therefore, according to the obtained results and the displacement of the band gap from the ultraviolet range to the visible light range, the energy required to excite the electron from the valence band to the conduction band and perform the sonocatalytic reaction is reduced and it is expected that the nanocatalyst synthesized in this study have more activity in presence of ultrasound waves.

3.5. Determining the effect of different initial pH values of sonocatalytic removal of ofloxacin and ciprofloxacin

In water and wastewater treatment, pH is an important factor in the removal of pollutants by adsorption and oxidation processes, so that it has a significant effect on the removal efficiency of pollutants [22]. Figs. 5 and 6 show the effect of pH on the degradation process of ofloxacin and ciprofloxacin at different levels of acid, neutral and alkali at different times and by keeping other variables constant. As shown in Fig. 5, the removal efficiency of ofloxacin increased at acidic pHs, so that it had the highest efficiency at pH = 3, and the removal efficiency decreased at alkaline and neutral pH value. In Fig. 6, at pH = 9, the highest removal efficiency of ciprofloxacin was observed.

Normally, the predominant surface electric charge on different types of catalysts may be positive or negative, depending on the surface properties, especially the functional groups of the surface and the components of the catalyst. In sonocatalytic processes, pHzpc plays an important role because, at pHzpc, the positive and negative electric charges on the catalyst surface are balanced. By increasing the pH above pHzpc, the dominant electric charge at the catalyst surface becomes negative, and by decreasing the pH below this point, the dominant electric charge at the catalyst surface becomes positive [23]. The pHzpc for titanium dioxide is between 5.6 and 6.4, so the surface of iron-doped titanium dioxide catalyst when pH <pHzpc is positive and pH > pHzpc is negative and is neutral at pH = pHzpc. On the other hand, the structural properties

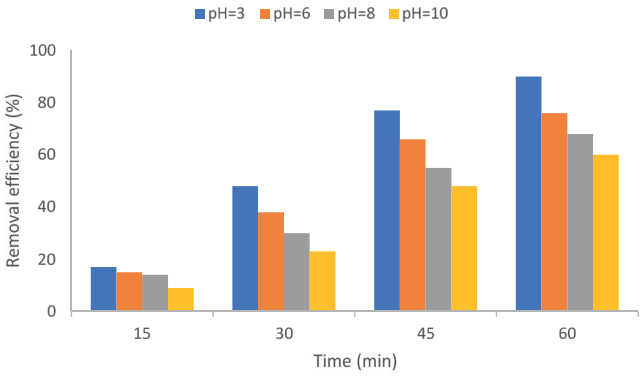

Fig. 5. Effect of initial pH on sonocatalytic removal of ofloxacin (initial concentration of ofloxacin = 100 mg/L and Fe-doped TiO_2 catalyst concentration = 500 mg/L).

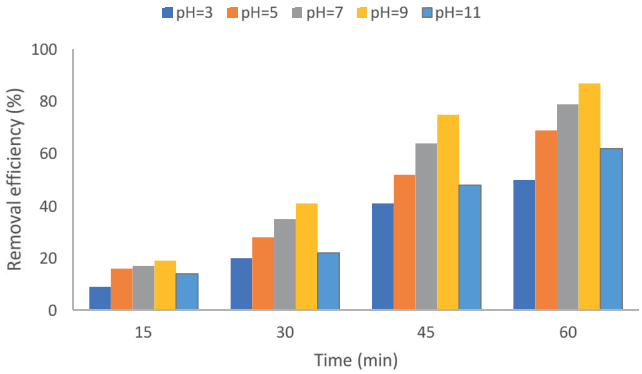

Fig. 6. Effect of initial pH on sonocatalytic removal of ciprofloxacin (initial concentration of ciprofloxacin = 100 mg/L and Fe-doped TiO_2 catalyst concentration = 500 mg/L).

of contaminants in the liquid environment and the formed intermediate products due to oxidation will change with changing pH. Various studies have shown that the attraction forces between the catalyst and ofloxacin increase under acidic conditions, which leads to an increase in the absorption of ofloxacin on the photocatalyst surface [9]. Bhatia et al. [4] and Hapeshi et al. [24], in their studies conducted for photocatalytic degradation of ofloxacin in aqueous solutions, have also obtained the maximum removal of ofloxacin at acidic pH.

Ofloxacin is mainly cationic below pKa1 (due to the presence of nitrogen in the position of the 4 piperazine groups), it is anionic and zoetrionic above pKa2 (due to the 6-carboxyl group), and it is neutral between pKa1 and pKa2. In this regard, the effect of solution pH on the sonocatalytic conversion of ofloxacin cannot be explained in terms of the ionization state of the substance and the catalyst because both have negative and positive charges in alkaline and acidic conditions, respectively [4,24]. Therefore, the differences shown in Fig. 5 may be due to the relative contribution of different reactions. At low pH values, positive holes are the main oxidation species due to the release of electrons into the conduction band, while at high pH and neutral conditions, hydroxyl radicals are considered the main species. As

the pH increases, the removal efficiency decreases, which may be due to the scavenging properties of the hydroxyl ions because the concentration of hydroxide ions (OH^-) increases with an increase in pH, and these hydroxide ions react with a number of effective hydroxyl radicals to form water molecules [4,24].

In acidic conditions, iron decomposes the compound in two direct (through reduction process) and indirect (through hydrogen production pathway due to iron oxidation) ways, both of which are better performed under acidic conditions. In addition, the Fenton-like process performs better in acidic conditions, which increases efficiency in acidic conditions [9].

The results of ciprofloxacin degradation in this study showed that the highest reaction rate constant of 0.38 min^{-1} is obtained at pH of 9, which is consistent with the results of An et al. [25] in the degradation of ciprofloxacin using the advanced oxidation process. Increasing the degradation efficiency at pH of 9 can be due to changes in the surface charge of nanoparticles at different pH values and with respect to pHzpc. On the other hand, ciprofloxacin exists in three different ionic forms, which mainly depend on the pH of the solution. The first degradation constant (pK1) of ciprofloxacin is 6.15, and the second degradation constant (pK2) is 8.66. In weakly alkaline conditions, large amounts of hydroxyl radicals can be produced by hydroxide ions. The constant reduction of the reaction at pH values above 9 may be due to the effect of repulsive forces and difficult absorption of negatively charged ciprofloxacin on the catalyst bed [25].

3.6. Determining the effect of initial concentration of ofloxacin and ciprofloxacin in the sonocatalytic removal process

Figs. 7 and 8 show the effect of initial concentrations of ofloxacin and ciprofloxacin on removal efficiencies, respectively. As the obtain results show, the maximum efficiency occurs at less initial concentration and decreases with increasing contaminant concentration.

The results of the studies conducted by Ayanda et al. [26] for sonocatalytic degradation of amoxicillin and the study performed by Zhao et al. [27] for the photocatalytic removal of ofloxacin were consistent with the results of this study. The reasons for the decrease in efficiency with increasing the initial concentration of the contaminant may be the following options: (1) As the concentration of the contaminant increases, more molecules are adsorbed on the surface of the nanocatalyst and therefore more radicals are needed to degrade the contaminant while under the same experimental conditions, radical production on the nanocatalyst surface is constant; hence, at high concentrations of contaminants, the existing reactive species are not sufficient for the degradation of the contaminants, therefore, the removal efficiency decreases with increasing concentration, and (2) Competition between pollutant molecules and degradation products increases with increasing pollutant concentration [26,27].

On the other hand, with increasing contaminant concentration, the ratio of shear stress produced by ultrasonic waves and active radicals that cause the degradation of the contaminant decreases [26]. In their study, Mohammadi et al. [28] showed that with increasing concentration of contaminants, more contaminant molecules adhere to the catalyst surface and the active sites of the catalyst decrease, so with increasing the occupied surface sites of the catalyst, the formation rate of hydroxyl radical ions are reduced. Sohrabnezhad et al. [29] also showed that increasing the concentration of contaminants in solution can lead to light absorption and reduce the number of photons reaching the surface of the catalyst, thereby reducing the excitation of nanoparticles and hydroxyl radicals.

3.7. Determining the effect of different amounts of Fe-doped TiO2 on sonocatalytic removal of ofloxacin and ciprofloxacin

One of the most important parameters affecting the efficiency and optimal performance of hybrid processes and catalytic oxidation is the dose of nanoparticles used in the process. Figs. 9 and 10 show the effect of different amounts of Fe-doped TiO2 nanoparticles on sonocatalytic removal of contaminants, which indicates an increase in removal efficiency with increasing concentration.

The study of He et al. [30] conducted for sonocatalytic degradation of orange acid 7 in aqueous media showed that by increasing the concentration of sonocatalyst particles to a certain extent, the efficiency of the process increases.

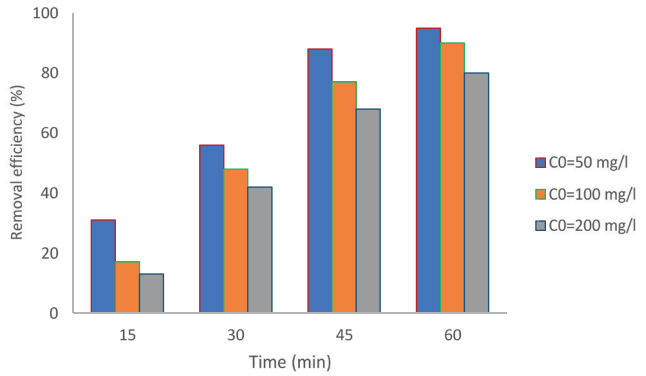

Fig. 7. Effect of initial concentration of ofloxacin on sonocatalytic removal of ofloxacin (pH = 3 and Fe-doped TiO_2 catalyst concentration = 500 mg/L).

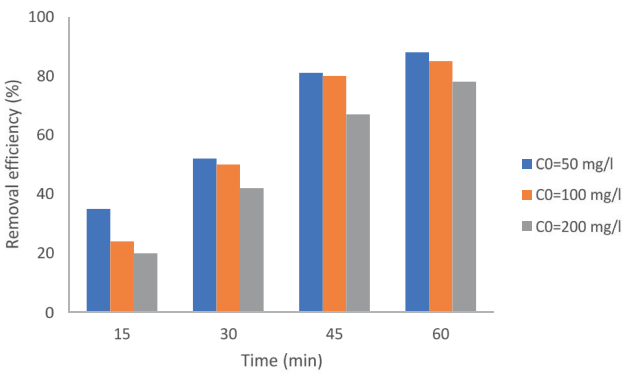

Fig. 8. Effect of initial ciprofloxacin concentration on sonocatalytic removal of ciprofloxacin (pH = 9 and Fe-doped TiO_2 catalyst concentration = 500 mg/L).

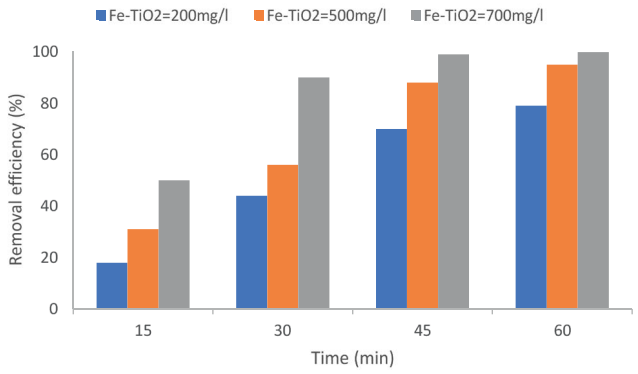

Fig. 9. Effect of different amounts of Fe-doped TiO_2 nanoparticles on sonocatalytic removal of ofloxacin (pH = 3, initial concentration of ofloxacin = 50 mg/L).

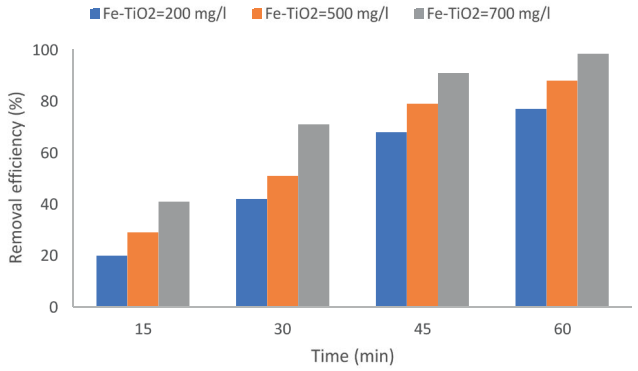

Fig. 10. Effect of different amounts of Fe-doped TiO_2 nanoparticles on sonocatalytic removal of ciprofloxacin (pH = 9, initial ciprofloxacin concentration = 50 mg/L).

This increase in sonocatalytic particles can provide more nuclei for the formation of cavitation bubbles, which in turn increases the production of hydroxyl radicals and further degradation of pollutants. On the other hand, increasing the amount of sonocatalyst in solution causes more increase of active sites for sonocatalytic reaction and production of more reactive oxygen species [30].

The results of the study conducted by Guo et al. [31] for degradation of flumequine by plasma along with graphene oxide/titanium dioxide nanocomposite showed that with increasing nanoparticle dose, the contact surface of the catalytic reaction is improved and more photons are converted to chemical energy by the plasma process produced, which accelerates the catalytic process [31].

The results of the study conducted by Hassani et al. [32] and Karim et al. [33] for the degradation of ciprofloxacin are consistent with the results of this study; based on their results, as the amount of catalyst increases, the number of active sites at the nanoparticle surface increases, and these nanoparticles form nucleation centers for the formation of cavitation bubbles, which in turn increase the production of hydroxyl radicals and reactive species, and greater amounts of contaminants are exposed to hydroxyl radicals and the removal efficiency increases.

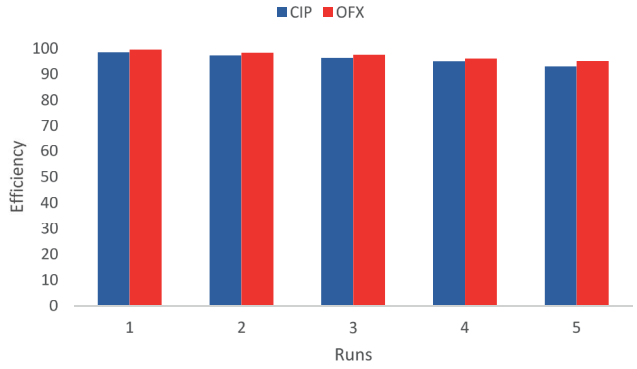

Fig. 11. Evaluation of stability and reusability of nanocatalysts in the degradation of ofloxacin and ciprofloxacin.

3.8. Evaluation of stability and reuse

One of the most important characteristics of catalysts in water and wastewater treatment processes is their reusability and stability in sequential applications. Therefore, Fe-doped TiO_2 nanocatalyst was separated from the solution after each oxidation step and used in the oxidation process after washing and re-drying. Fig. 11 displays the sonocatalytic degradation efficiency of nanoparticles after five reuse. The obtained results show that after reuse, the removal efficiency is slightly reduced, which can be due to the blockage of surface active sites by intermediates of ciprofloxacin, destruction of nanocatalysts by degradation products, reduction of catalyst ability during washing and drying processes. In addition, after separating Fe-doped TiO_2 nanoparticles from the oxidized effluent, to determine the amount of iron and titanium elements released in solution, the concentration of the above elements was analyzed by ICP-MS and the results showed that the concentration of the above-mentioned elements cannot be measured in filtered effluent, which is indicative of the stability of synthesized nanoparticles.

3.9. Reaction kinetics

The removal kinetics of many organic compounds are interpreted using the Langmuir–Hinshelwood kinetic model, which is used to express the relationship between the initial degradation rate and the initial concentration of organic compounds in sonocatalytic degradation reactions. The equation used by the Langmuir-Hinshelwood model is as follows:

$$\frac{1}{K_{obs}} = \frac{1}{k_c k_{LH}} + \frac{C_0}{k_c} \tag{4}$$

where C_0 reveals the initial concentration of the antibiotics (mg. L^{-1}), k_{LH} is the equilibrium constant of the Langmuir–Hinshelwood model, and k_c is the constant rate of surface reaction rate (mg/L min). In cases where the pollutant concentration is low ($C = C_0$ at $t = 0$), the above equation becomes simpler and is expressed as a first-order equation as follows:

$$r = -\frac{dc}{dt} = k_{obs} C \tag{5}$$

$$\ln\left(\frac{C_0}{C_t}\right) = k_{obs}t \quad (6)$$

where r (mg/L min) is indicative of sonocatalytic reduction rate of ofloxacin and ciprofloxacin antibiotics in the initial reaction times; $C = C_0$ (mg/L) is the initial concentration of ofloxacin and ciprofloxacin antibiotics, and k_{obs} (L/mg) represents the constant apparent rate of first-order oxidation, which is affected by antibiotics concentrations. By plotting $\ln(C_0/C_t)$ against time, the value of k_{obs} and the correlation coefficient can be determined for different concentrations. When $\ln(C_0/C_t)$ is plotted against time, a straight line is obtained whose the apparent rate constant of pseudo-first-order kinetics (k_{obs}) is the slope of the line [4].

The degradation kinetics of ofloxacin and ciprofloxacin are shown in Table 2. As can be seen, the rate constant of reaction was the highest at pH of 3 and 9, the catalyst dose of 700 mg/L, and the pollutant concentration of 50 mg/L, which confirms the results of the previous graphs.

3.10. Proposed pathway and mechanism for the degradation of ofloxacin and ciprofloxacin

The degradation products in different photocatalytic, sonocatalytic, and sonophotocatalytic processes may be identical and similar. Vasquez et al. [34] proposed two main pathways for producing the degradation by-products of ofloxacin by photolytic and photocatalytic processes as follows: piperazine ring dealkylation and decarboxylation (carboxyl group deletion, –COOH) [34]. Studies have shown that fluoroquinolones lose their fluoride during major photolytic reactions, and after that, decarboxylation occurs. By oxidizing the pyrazine ring of ofloxacin, a product with 291 m/z is produced. By cleavage of $C_{11}H_{15}FN_2$, the intermediate with 169 m/z is formed and again, with the loss of a methyl group, the intermediate with 157 m/z is formed [35].

The usual route of ciprofloxacin degradation is to attack the carboxyl and fluorine groups. The degradation pathway proposed by Karim et al. [33] shows that further decomposition of the fluorine group forms female ions with 228.15 m/z (*I*). After carboxylic cleavage from the quinolone region, intermediate compound *I* is oxidized to compound *J* [33]. On the other pathway, after decarboxylation of ciprofloxacin, the intermediate product *E* is formed with the same m/z equal to 288.15 which with further decomposition leads to the separation of the quinolone part and the formation of the product in the form of *K* [33]. On the other hand, by adding the mono-hydroxyl group to the main compound of ciprofloxacin, the intermediate product *L* with 348 m/z is formed, which has been reported by An et al. [25].

In the case of advanced oxidation processes, it is noteworthy that hydroxyl radicals attack organic compounds selectively, so it is not possible to identify all the products produced [35].

According to a study by Shen et al. [36], the molecular structure of fluoroquinolones is responsible for binding the drug to bacterial DNA. Therefore, it is expected that the antimicrobial activity of the drug will decrease only when this part of the structure is destroyed [35,36]. However, even if the by-products of decomposition of a quinolone nucleus are intact, their antimicrobial activity is lower. This suggests that changes in adjuvant functional groups can also reduce antimicrobial activity. The ofloxacin piperazine ring is responsible for identifying and binding the drug to DNA enzymes of bacterial topoisomerase. Therefore, the by-product with 291 m/z, which has structural fragmentation, is less prone to the target bacterium and has less antimicrobial activity than the main compound [35].

Fluoroquinolones require the carboxyl group (–COOH) to function. Therefore, the proposed by-product with 157 m/z has no antimicrobial activity [35].

Paul et al. showed that there was a significant reduction (more than 90%) in the antimicrobial activity of ciprofloxacin solutions under UV/ H_2O_2 and photocatalysis [37].

The main mechanism of US waves in the oxidation of pollutants is the formation of tiny holes or microbubbles that are caused by the phenomenon of sound cavitation.

Table 2
The effect of different variables on the degradation kinetics of ofloxacin and ciprofloxacin

Parameter	CIP				OFX			
	Value of variable	$k_0 \times 10^{-2}$ (min^{-1})	R^2	$t_{1/2}$ (min)*	Value of variable	$k_0 \times 10^{-2}$ (min^{-1})	R^2	$t_{1/2}$ (min)*
Initial pH	3	1.21	0.96	57.27	3	3.93	0.94	17.63
	5	1.93	0.95	35.90	6	2.51	0.96	27.60
	7	2.64	0.95	26.25	8	1.95	0.96	35.53
	9	3.5	0.94	19.8	10	1.59	0.95	43.58
	11	1.63	0.94	42.51				
Ciprofloxacin (mg/L)	5	3.65	0.97	18.98	5	5.16	0.95	13.43
	15	3.42	0.96	20.26	15	3.93	0.94	17.63
	20	2.61	0.98	26.55	20	2.81	0.96	24.66
Fe-doped TiO_2 (mg/L)	200	2.57	0.97	26.96	200	2.75	0.97	25.2
	500	3.64	0.97	19.03	500	5.16	0.94	13.43
	700	6.85	0.94	10.11	700	11.82	0.96	5.86

*$t_{1/2}$ (min) = 0.693/k_0.

In the sonocatalytic process, the phenomenon of sonoluminescence and hotspots caused by sonic cavitation leads to the production of short-wavelength light (<420 nm), which is a source of energy for catalytic activity and produces electron-hole pairs at the nanocatalyst surface [Eq. (7)]. The produced holes (h^+) can degrade the pollutant directly by reacting with the pollutants in the environment or indirectly by decomposing the water molecules and producing active radicals [Eq. (8)]. The generated electrons can also produce the hydroxyl radicals after the reaction [Eqs. (9) and (10)]. By doping Fe^{3+} to the TiO_2 structure, it creates a new intermediate surface in the conduction layer of TiO_2 so that the excited electrons can react with Fe^{3+} and prevent the recombination of electron and the hole, and as a result, increasing the efficiency. The production and trapping of the generated charges were presented in Eqs. (11)–(14). As a result, these produced radicals cause the degradation of ciprofloxacin, ofloxacin and its intermediates into final CO_2, H_2O, and mineral products [Eq. (15)].

$$\text{Sonocataly} + \text{US} \rightarrow h^+ + e^- \tag{7}$$

$$h^+ + H_2O \rightarrow {}^{\bullet}OH + H^+ \tag{8}$$

$$e^- + O_2 \rightarrow O_2^{\bullet -} \tag{9}$$

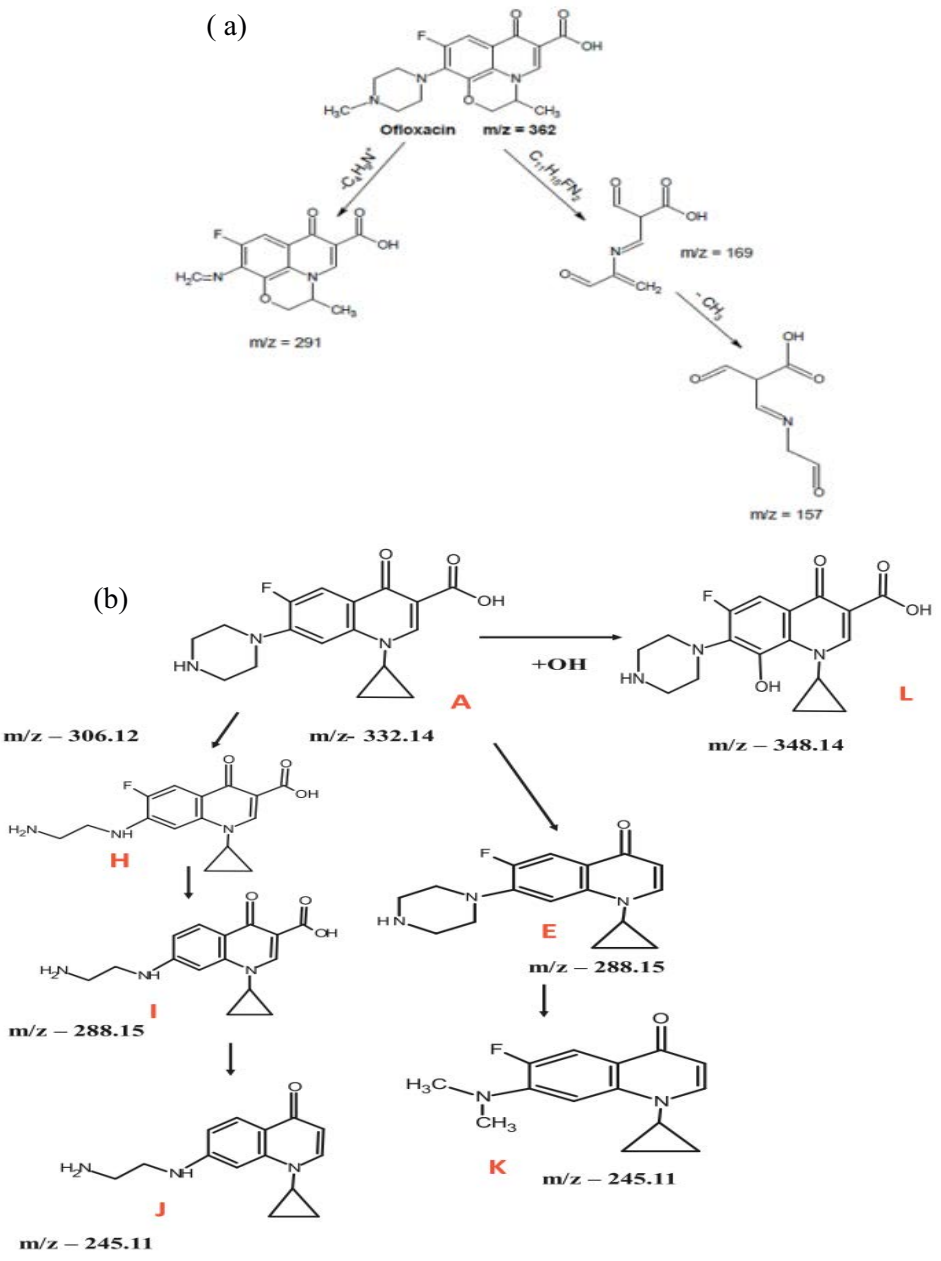

Fig. 12. Degradation pathway proposed for ofloxacin by Peres et al. [35] (a) and ciprofloxacin by Karim et al. [33] (b).

$$H_2O_2 + O_2^{\bullet -} \rightarrow {}^{\bullet}OH + OH^- + O_2 \quad (10)$$

$$Fe^{3+} + e_{CB}^- \rightarrow Fe^{2+}\left(\text{Electron trap}\right) \quad (11)$$

$$Fe^{2+} + Ti^{4+} \rightarrow Fe^{3+} + Ti^{3+}\left(\text{Migration}\right) \quad (12)$$

$$Fe^{3+} + h_{VB}^+ \rightarrow Fe^{4+}\left(\text{Hole trap}\right) \quad (13)$$

$$Fe^{4+} + OH^- \rightarrow Fe^{3+} + {}^{\bullet}OH\left(\text{Migration}\right) \quad (14)$$

$$\text{Cip \& Ofl} + {}^{\bullet}OH \rightarrow \text{Intermediates} \rightarrow H_2O + CO_2 + \text{Inorganic species} \quad (15)$$

4. Conclusion

This study was performed to evaluate the efficiency of sonocatalytic oxidation for removal of ofloxacin and ciprofloxacin by Fe-doped TiO_2 nanoparticles from aqueous solution. SEM, EDX, XRD, and DRS analyses were used to determine the properties of the synthesized nanoparticles. Analyses showed that the synthesized particles by the sol-gel method are very fine and have good uniformity and dispersion. The results of EDX showed the presence of Ti, Fe, and O elements in the structure of synthesized nanocatalyst and also confirm the doping process of synthesized nanoparticles. In XRD analysis, the presence of large and sharp peaks confirms the fine crystal structure of the synthesized nanoparticles. Doping iron in the structure of titanium dioxide causes the absorption wavelength to shift to higher wavelengths and get closer to the visible region. The maximum removal efficiency of ofloxacin and ciprofloxacin using ultrasound frequency of 35 kHz under optimal conditions including the initial contaminant concentration of 50 mg/L, the doped nanoparticle dosage of 700 mg/L during the reaction time of 60 min were obtained at pH values of 3 and 9, respectively. Sonocatalytic analysis of antibiotics followed the first-order kinetic model. The synthesized nanoparticles have reasonable catalytic stability and have a relatively small reduction in catalytic activity for the degradation of antibiotics. Therefore, due to the high efficiency of the sonocatalytic process, good stability, and the possibility of reuse of synthesized nanoparticles, the use of this process is recommended to remove ofloxacin, ciprofloxacin, and other resistant contaminants in complimentary water and wastewater treatment processes.

Acknowledgment

This article is the result of a part of the Ph.D. thesis of Islamic Azad University, Science and Research Branch of Tehran. The Islamic Azad University, Science and Research Branch of Tehran is hereby thanked for the financial and spiritual support of this research.

Conflicts of interest/Competing interests

The authors declare that they have no competing interests.

References

[1] E. Norabadi, A.H. Panahi, R. Ghanbari, A. Meshkinian, H. Kamani, S.D. Ashrafi, Optimizing the parameters of amoxicillin removal in a photocatalysis/ozonation process using Box–Behnken response surface methodology, Desal. Water Treat., 192 (2020) 234–240.

[2] A.H. Panahi, S.D. Ashrafi, H. Kamani, M. Khodadadi, E.C. Lima, F.K. Mostafapour, A.H. Mahvi, Removal of cephalexin from artificial wastewater by mesoporous silica materials using Box–Behnken response surface methodology, Desal. Water Treat., 159 (2019) 169–180.

[3] Q. Su, J. Li, H. Yuan, B. Wang, Y. Wang, Y. Li, Y. Xing, Visible-light-driven photocatalytic degradation of ofloxacin by g-C_3N_4/NH_2-MIL-88B(Fe) heterostructure: mechanisms, DFT calculation, degradation pathway and toxicity evolution, Chem. Eng. J., 427 (2022) 131594, doi: 10.1016/j.cej.2021.131594.

[4] V. Bhatia, A.K. Ray, A. Dhir, Enhanced photocatalytic degradation of ofloxacin by co-doped titanium dioxide under solar irradiation, Sep. Purif. Technol., 161 (2016) 1–7.

[5] S.-L. Liu, B. Liu, Z. Xiang, L. Xu, X.-F. Wang, Y. Liu, X. Wang, Fabrication of $CaWO_4$ microspheres with enhanced sonocatalytic performance for ciprofloxacin removal in aqueous solution, Colloids Surf., A, 628 (2021) 127206, doi: 10.1016/j.colsurfa.2021.127206.

[6] A. Jahantiq, R. Ghanbari, A. Hossein Panahi, S.D. Ashrafi, A.D. Khatibi, E. Noorabadi, A. Meshkinian, H. Kamani, Photocatalytic degradation of 2,4,6-trichlorophenol in aqueous solutions using synthesized Fe-doped TiO_2 nanoparticles via response surface methodology, Desal. Water Treat., 183 (2020) 366–373.

[7] H. Kamani, S. Nasseri, M. Khoobi, R.N. Nodehi, A.H. Mahvi, Sonocatalytic degradation of humic acid by N-doped TiO_2 nano-particle in aqueous solution, J. Environ. Health Sci. Eng., 14 (2016) 3, doi: 10.1186/s40201-016-0242-2.

[8] H. Kamani, S.D. Ashrafi, A. Jahantiq, E. Norabadi, M. Dashti Zadeh, Catalytic degradation of humic acid using Fe–doped TiO_2 - ultrasound hybrid system from aqueous solution, Int. J. Environ. Anal. Chem., (2021) 1–15, doi: 10.1080/03067319.2021.1979535.

[9] E. Norabadi, S.D. Ashrafi, H. Kamani, A. Jahantiq, Degradation of 2,6-dichlorophenol by Fe-doped TiO_2 Sonophotocatalytic process: kinetic study, intermediate product, degradation pathway, Int. J. Environ. Anal. Chem., (2020) 1–16, doi: 10.1080/03067319.2020.1837122.

[10] E. Hapeshi, I. Fotiou, D. Fatta-Kassinos, Sonophotocatalytic treatment of ofloxacin in secondary treated effluent and elucidation of its transformation products, Chem. Eng. J., 224 (2013) 96–105.

[11] M. Pirsaheb, B. Shahmoradi, T. Khosravi, K. Karimi, Y. Zandsalimi, Solar degradation of malachite green using nickel-doped TiO_2 nanocatalysts, Desal. Water Treat., 57 (2016) 9881–9888.

[12] C.P. Sajan, B. Shahmoradi, H.P. Shivaraju, K.M.L. Rai, S. Ananda, M.B. Shayan, T. Thonthai, G.V.N. Rao, K. Byrappa, Photocatalytic degradation of textile effluent using hydrothermally synthesised titania supported molybdenum oxide photocatalyst, Mater. Res. Innov., 14 (2010) 89–94.

[13] J. Wang, W. Sun, Z. Zhang, Z. Jiang, X. Wang, R. Xu, R. Li, X. Zhang, Preparation of Fe-doped mixed crystal TiO_2 catalyst and investigation of its sonocatalytic activity during degradation of azo fuchsine under ultrasonic irradiation, J. Colloid Interface Sci., 320 (2008) 202–209.

[14] K. Salehi, B. Shahmoradi, A. Bahmani, M. Pirsaheb, H.P. Shivaraju, Optimization of reactive black 5 degradation using hydrothermally synthesized NiO/TiO_2 nanocomposite under natural sunlight irradiation, Desal. Water Treat., 57 (2016) 25256–25266.

[15] B. Shahmoradi, I.A. Ibrahim, N. Sakamoto, S. Ananda, T.N. Row, K. Soga, K. Byrappa, S. Parsons, Y. Shimizu, In situ surface modification of molybdenum-doped organic-inorganic hybrid TiO_2 nanoparticles under hydrothermal conditions and treatment of pharmaceutical effluent, Environ. Technol., 31 (2010) 1213–1220.
[16] B. Shahmoradi, M.A. Pordel, M. Pirsaheb, A. Maleki, S. Kohzadi, Y. Gong, R.R. Pawar, S.-M. Lee, H.P. Shivaraju, G. McKay, Synthesis and characterization of barium-doped TiO_2 nanocrystals for photocatalytic degradation of Acid Red 18 under solar irradiation, Desal. Water Treat., 88 (2017) 200–206.
[17] S.I. Abbas, H.T. John, A.J. Fraih, Technology, Preparation of nano crystalline zinc–ferrite as material for microwaves absorption by sol–gel methods, Indian J. Sci. Technol., 10 (2017) 1–6.
[18] L. Liu, F. Chen, F. Yang, Y. Chen, J. Crittenden, Photocatalytic degradation of 2,4-dichlorophenol using nanoscale Fe/TiO_2, Chem. Eng. J., 181–182 (2012) 189–195.
[19] Y.L. Pang, A.Z. Abdullah, Effect of low Fe^{3+} doping on characteristics, sonocatalytic activity and reusability of TiO_2 nanotubes catalysts for removal of Rhodamine B from water, J. Hazard. Mater., 235 (2012) 326–335.
[20] V. Moradi, M.B. Jun, A. Blackburn, R.A. Herring, Significant improvement in visible light photocatalytic activity of Fe doped TiO_2 using an acid treatment process, Appl. Surf. Sci., 427 (2018) 791–799.
[21] Y. Sui, Q. Liu, T. Jiang, Y. Guo, Synthesis of nano-TiO_2 photocatalysts with tunable Fe doping concentration from Ti-bearing tailings, Appl. Surf. Sci., 428 (2018) 1149–1158.
[22] H. Kamani, G.H. Safari, G. Asgari, S.D. Ashrafi, Data on modeling of enzymatic elimination of Direct Red 81 using response surface methodology, Data Brief, 18 (2018) 80–86.
[23] H. Kamani, E. Bazrafshan, S.D. Ashrafi, F. Sancholi, Efficiency of sono-nano-catalytic process of TiO_2 nano-particle in removal of erythromycin and metronidazole from aqueous solution, J. Mazandaran Univ. Med. Sci., 27 (2017) 140–154.
[24] E. Hapeshi, A. Achilleos, M.I. Vasquez, C. Michael, N.P. Xekoukoulotakis, D. Mantzavinos, D. Kassinos, Drugs degrading photocatalytically: kinetics and mechanisms of ofloxacin and atenolol removal on titania suspensions, J. Water Res., 44 (2010) 1737–1746.
[25] T. An, H. Yang, G. Li, W. Song, W.J. Cooper, X. Nie, Kinetics and mechanism of advanced oxidation processes (AOPs) in degradation of ciprofloxacin in water, Appl. Catal., B, 94 (2010) 288–294.
[26] O.S. Ayanda, O.H. Aremu, C.O. Akintayo, K.O. Sodeinde, W.N. Igboama, E.O. Oseghe, S.M. Nelana, Sonocatalytic degradation of amoxicillin from aquaculture effluent by zinc oxide nanoparticles, Environ. Nanotechnol. Monit. Manage., 16 (2021) 100513, doi: 10.1016/j.enmm.2021.100513.
[27] G. Zhao, J. Ding, F. Zhou, X. Chen, L. Wei, Q. Gao, K. Wang, Q. Zhao, Construction of a visible-light-driven magnetic dual Z-scheme $BiVO_4$/g-C_3N_4/$NiFe_2O_4$ photocatalyst for effective removal of ofloxacin: mechanisms and degradation pathway, Chem. Eng. J., 405 (2021) 126704, doi: 10.1016/j.cej.2020.126704.
[28] R. Mohammadi, B. Massoumi, M. Rabani, Photocatalytic decomposition of amoxicillin trihydrate antibiotic in aqueous solutions under UV irradiation using Sn/TiO_2 nanoparticles, Int. J. Photoenergy, 2012 (2012), doi: 10.1155/2012/514856.
[29] S. Sohrabnezhad, Study of catalytic reduction and photodegradation of methylene blue by heterogeneous catalyst, Spectrochim. Acta, Part A, 81 (2011) 228–235.
[30] L.-L. He, Y. Zhu, Q. Qi, X.-Y. Li, J.-Y. Bai, Z. Xiang, X. Wang, Synthesis of $CaMoO_4$ microspheres with enhanced sono-catalytic performance for the removal of Acid Orange 7 in the aqueous environment, Sep. Purif. Technol., 276 (2021) 119370, doi: 10.1016/j.seppur.2021.119370.
[31] H. Guo, N. Jiang, H. Wang, K. Shang, N. Lu, J. Li, Y. Wu, Degradation of flumequine in water by pulsed discharge plasma coupled with reduced graphene oxide/TiO_2 nanocomposites, Sep. Purif. Technol., 218 (2019) 206–216.
[32] A. Hassani, A. Khataee, S. Karaca, C. Karaca, P. Gholami, Sonocatalytic degradation of ciprofloxacin using synthesized TiO_2 nanoparticles on montmorillonite, Ultrason. Sonochem., 35 (2017) 251–262.
[33] A.V. Karim, A. Shriwastav, Degradation of ciprofloxacin using photo, sono, and sonophotocatalytic oxidation with visible light and low-frequency ultrasound: degradation kinetics and pathways, Chem. Eng. J., 392 (2020) 124853, doi: 10.1016/j.cej.2020.124853.
[34] M.I. Vasquez, M. Garcia-Käufer, E. Hapeshi, J. Menz, K. Kostarelos, D. Fatta-Kassinos, K. Kümmerer, Chronic ecotoxic effects to *Pseudomonas putida* and *Vibrio fischeri*, and cytostatic and genotoxic effects to the hepatoma cell line (HepG2) of ofloxacin photo(cata)lytically treated solutions, Sci. Total Environ., 450–451 (2013) 356–365.
[35] M.S. Peres, M.G. Maniero, J.R. Guimarães, Photocatalytic degradation of ofloxacin and evaluation of the residual antimicrobial activity, Photochem. Photobiol. Sci., 14 (2015) 556–562.
[36] L.L. Shen, J. Baranowski, A.G. Pernet, Mechanism of inhibition of DNA gyrase by quinolone antibacterials: specificity and cooperativity of drug binding to DNA, Biochemistry, 28 (1989) 3879–3885.
[37] T. Paul, M.C. Dodd, T.J. Strathmann, Photolytic and photocatalytic decomposition of aqueous ciprofloxacin: transformation products and residual antibacterial activity, Water Res., 44 (2010) 3121–3132.